

# Synergistic Effect of Cobalt Oxide-Graphitic Carbon Nitride Nanocomposite for Visible Light Driven Degradation of Crystal Violet Dye

Pramod Ugale<sup>1</sup>; Paras Tak<sup>2</sup>; Rameshwar Ameta<sup>3</sup>

<sup>1</sup>Research Scholar, PAHER University, Udaipur, Rajasthan, India.

<sup>2</sup>Professor, PAHER University, Udaipur, Rajasthan, India.

<sup>3</sup>Professor, PAHER University, Udaipur, Rajasthan, India.

Publication Date: 2026/05/27

**Abstract:** To combat the growing issue of dye contamination in wastewater, developing high-performance photocatalysts is essential. This research details the fabrication of cobalt oxide-graphitic carbon nitride ( $\text{Co}_3\text{O}_4/\text{g-C}_3\text{N}_4$ ) nanocomposites, achieved through a straightforward, single-step pyrolysis process utilizing urea as the  $\text{g-C}_3\text{N}_4$  precursor. Comprehensive material characterization was conducted using X-ray diffraction (XRD), field emission scanning electron microscopy (FESEM), and energy-dispersive X-ray spectroscopy (EDX). The resulting data verified successful cobalt oxide integration, a crystalline framework, and a unique flower-like structural morphology featuring a mean crystallite size of 89.14 nm. The performance of the fabricated nanocomposite was tested by measuring how effectively it breaks down Crystal violet dye under visible light. During this evaluation, the team systematically adjusted key variables, including light intensity, catalyst amount, initial dye concentration, and pH levels. The results revealed that the composite performs significantly better than either pure cobalt oxide or standalone  $\text{g-C}_3\text{N}_4$ . This boosted efficiency stems from a clear synergistic interaction, which improves charge separation and strengthens interfacial contact. Consequently, these outcomes highlight the potential of  $\text{Co}_3\text{O}_4/\text{g-C}_3\text{N}_4$  nanocomposites as highly effective agents for eco-friendly wastewater treatment.

**Keywords:** Photocatalyst, Nanocomposite, Synergistic Effect, Cobalt Oxide,  $\text{g-C}_3\text{N}_4$ , Dye Degradation.

**How to Cite:** Pramod Ugale; Paras Tak; Rameshwar Ameta (2026) Synergistic Effect of Cobalt Oxide-Graphitic Carbon Nitride Nanocomposite for Visible Light Driven Degradation of Crystal Violet Dye. *International Journal of Innovative Science and Research Technology*, 11(5), 1842-1851. <https://doi.org/10.38124/ijisrt/26may1044>

## I. INTRODUCTION

Synthetic dyes are widely used in textile, paper, leather, and food industries, and their discharge into aquatic systems has become a major environmental concern. These dyes are often non-biodegradable, toxic, and resistant to conventional treatment methods, leading to persistent contamination of water bodies and posing risks to both ecosystems and human health. Therefore, the development of efficient and sustainable methods for dye removal has become a pressing research priority.

Using light irradiation to break down intricate organic contaminants into safe end products has made photocatalysis a leading strategy for purifying wastewater. Graphitic carbon nitride ( $\text{g-C}_3\text{N}_4$ ) stands out among diverse photocatalytic materials for its visible-light responsiveness, chemical resilience, and metal-free composition. Despite these benefits, its overall performance is constrained by the swift recombination of electron-hole pairs. Similarly, while the transition metal oxide cobalt oxide ( $\text{Co}_3\text{O}_4$ ) offers outstanding redox characteristics, its real-world utility is obstructed by

poor light absorption and low standalone photocatalytic performance.

To overcome these limitations, combining  $\text{g-C}_3\text{N}_4$  with  $\text{Co}_3\text{O}_4$  into a nanocomposite provides a synergistic effect, enhancing charge separation, extending light absorption, and improving overall photocatalytic efficiency. In this study, we report the synthesis of  $\text{Co}_3\text{O}_4/\text{g-C}_3\text{N}_4$  nanocomposites via a simple one-step pyrolysis method using urea as the precursor for  $\text{g-C}_3\text{N}_4$ . The structural and morphological features of the nanocomposites were characterized, and their photocatalytic performance was systematically evaluated for dye degradation under visible light. The results demonstrate that the nanocomposite exhibits superior activity compared to the individual components, establishing its potential as a sustainable photocatalyst for wastewater remediation.

## II. LITERATURE REVIEW

Synthetic dyes are widely used in industries such as textiles, paper, leather, and food processing due to their engineered resistance to fading. However, this very stability

makes them non-biodegradable, allowing them to persist in the environment for long periods [1]. Beyond their persistence, many synthetic dyes pose direct risks to living organisms. They have been reported to exhibit mutagenic and carcinogenic properties, and their tendency to bioaccumulate in aquatic species further amplifies ecological and health hazards [2]. Researchers have explored various strategies to overcome these challenges, including the use of co-catalysts, dopants, and composites [3]. Titanium dioxide (TiO<sub>2</sub>) is the most widely studied photocatalyst due to its abundance, low cost, and stability under UV light. As a wide-bandgap semiconductor (3.2 eV), its activity is limited to UV excitation, restricting solar applications. While TiO<sub>2</sub> is chemically stable, non-toxic, and highly active under UV, doping with metals (Pt, Au) or non-metals (N, C) can enhance efficiency by narrowing the bandgap, improving charge separation, and extending light absorption [4]. Graphitic carbon nitride (g-C<sub>3</sub>N<sub>4</sub>)-based Z-scheme heterojunctions are promising photocatalysts for solar energy conversion and environmental remediation. Their enhanced performance arises from efficient photocarrier separation, strong visible-light response, and spatially separated redox sites, leading to significantly improved photocatalytic activity [5]. Semiconductor-based photocatalysis is regarded as a promising solution to the global energy crisis and environmental degradation. Since 2009, the pioneering work on graphitic carbon nitride (g-C<sub>3</sub>N<sub>4</sub>) for visible-light photocatalytic water splitting has been a very hot research topic [6]. The distinct nanostructure of g-C<sub>3</sub>N<sub>4</sub> allows for metal modifications that yield advanced metal-semiconductor configurations. By integrating metals, the photochemical properties of g-C<sub>3</sub>N<sub>4</sub> are shifted; specifically, the bandgap narrows and light absorption extends further into the visible spectrum, thereby maximizing photocatalytic performance [7]. Despite these possibilities, unmodified g-C<sub>3</sub>N<sub>4</sub> delivers only mediocre photocatalytic results due to rapid charge carrier recombination and a restricted specific surface area. To overcome these limitations, porous carbon nitride (PCN) has gained prominence among altered g-C<sub>3</sub>N<sub>4</sub> variants; its configuration expands specific surface areas, introduces more active surface sites, enhances light-harvesting, and boosts overall adsorption, activation, and diffusion [8]. Exploring alternative composites, An et al. engineered a zinc oxide-functionalized graphitic carbon nitride matrix designed to break down aqueous organic pollutants. Their method involved synthesizing ZnO via calcination using *Garcinia mangostana* pericarp extract as a stabilizing and reducing agent, while the g-C<sub>3</sub>N<sub>4</sub> component was calcinated and subsequently stripped via strong chemical oxidation. This resulting zinc-carbon nitride composite (ZCN) proved highly versatile, successfully degrading malachite green (MG) and methyl orange (MO) dyes at efficiencies of 96.42% and 57.57%, respectively [9].

Using an accessible and economical sol-gel approach, Dhas et al. fabricated cobalt oxide nanoparticles, integrating triethanolamine (TEA) as a surfactant to control and minimize particle dimensions. Their optical analysis revealed dual energy bandgaps stemming from distinct electronic transitions, while photoluminescence spectroscopy indicated that the presence of the TEA surfactant successfully

minimized structural defects. These synthesized nanoparticles were then employed to catalyse the ultraviolet-light-driven breakdown of Direct Red 80 and Rhodamine B dyes. In a separate study, Farhadi et al. explored the solid-state thermal decomposition of a [Co(NH<sub>3</sub>)<sub>5</sub>(H<sub>2</sub>O)](NO<sub>3</sub>)<sub>3</sub> precursor complex. The resulting Co<sub>3</sub>O<sub>4</sub> nanoparticles displayed two optical absorption bandgaps at 2.20 eV and 3.45 eV, validating their semiconducting nature and showing strong photocatalytic efficiency when breaking down methylene blue (MB) under visible light [11]. Furthermore, Asif et al. developed a solar-driven photocatalyst composed of Co<sub>3</sub>O<sub>4</sub>/Fe<sub>2</sub>O<sub>3</sub> composite nanofibers. This material achieved rapid degradation of brilliant cresyl blue (BCB) and acridine orange (AO) under sunlight, with the highest catalytic efficiency observed in alkaline (high pH) environments. Kinetic modelling of the AO and BCB breakdown confirms that this nanofiber composite represents a highly capable solar photocatalyst for eliminating toxic and hazardous organic pollutants [12].

Employing an eco-friendly aqueous bi-thermal technique, Pattnaik et al. synthesized nano-exfoliated g-C<sub>3</sub>N<sub>4</sub>. This material was subsequently used to evaluate the ultraviolet-light-driven degradation of ciprofloxacin (CPN) in an aqueous environment. The resulting exfoliated g-C<sub>3</sub>N<sub>4</sub> yielded a surface area nearly three times larger than its bulk counterpart, translating into a two-and-a-half-fold increase in photocatalytic performance. This enhanced behaviour is attributed to the expanded surface area, which successfully promotes charge carrier separation and curtails the recombination of photogenerated pairs. The researchers thoroughly examined how initial CPN concentrations, irradiation times, and catalyst dosages influenced the degradation process, noting that a 1 g/L concentration of nano-exfoliated g-C<sub>3</sub>N<sub>4</sub> successfully broke down 78% of a 20 ppm CPN solution within one hour of sunlight exposure [13]. In another study, Cui et al. developed hollow graphitic carbon nitride (g-C<sub>3</sub>N<sub>4</sub>) spheres using a template-free, single-step solvothermal approach. They systematically investigated how varying condensation temperatures influenced the structural, optical, and photocatalytic attributes of the material. Their data indicated that elevated condensation temperatures boost both visible-light harvesting and the migration velocity of photo-induced charge carriers. Ultimately, the g-C<sub>3</sub>N<sub>4</sub> matrix synthesized at 180 °C demonstrated the peak photocatalytic efficiency when degrading Rhodamine B (RhB) under visible light [14].

Alshamsi et al. evaluated the photo-decolorization kinetics of Crystal Violet (CV) by comparing a UV/H<sub>2</sub>O<sub>2</sub> system against Fenton's reagent. When exposed to either H<sub>2</sub>O<sub>2</sub> or ultraviolet light independently, the dye showed negligible degradation. The Fenton-driven system broke down the colour far more rapidly than the photolytic route, yet the overall degree of decolorization proved to be entirely unaffected by variations in pH. Beyond establishing a tentative degradation pathway, the researchers tracked how ambient anions typically present in industrial dye discharge affect the treatment process. Their analysis revealed an unexpected finding: hydrogen phosphate ions heavily suppressed the Fenton-mediated decolorization mechanism

while exercising a minimal influence on the parallel photolytic degradation pathway [15]. Sahoo et al. examined how effectively silver-doped titanium dioxide degrades Crystal Violet a triphenylmethane-based dye in an aqueous environment under both ultraviolet and simulated solar irradiation. To track the complete mineralization of the contaminant, chemical oxygen demand (COD) levels were systematically recorded at fixed time intervals. The study comprehensively mapped how dye breakdown is influenced by operational parameters, including solution pH, catalyst concentration, and initial substrate loading, alongside common matrix interferences such as humic acid and various ionic species  $\text{Cl}^-$ ,  $\text{HPO}_4^{2-}$ ,  $\text{Ca}^{2+}$ ,  $\text{Fe}^{3+}$ ,  $\text{NO}_3^-$ ,  $\text{SO}_4^{2-}$ . Under UV exposure for 105 minutes, a 20 ppm dye solution achieved over 97% degradation using pristine  $\text{TiO}_2$ , whereas doping the catalyst with silver  $\text{Ag}^+$  pushed the overall decomposition efficiency beyond 99%. [16]. Ahmad et al. developed an innovative bismuth-iron selenide photocatalyst using a solvothermal synthesis approach specifically targeting the breakdown of hazardous, carcinogenic crystal violet dye. To optimize its utility, the catalyst was anchored onto a chitosan matrix, yielding iron-bismuth selenide-chitosan microspheres designated as BISE-CM. Under idealized solar irradiation conditions, this composite framework demonstrated vastly elevated degradation performance toward the target dye. Specifically, using a 0.2 g dosage of the BISE-CM catalyst at an alkaline pH of 8.0, a 30 ppm crystal violet dye solution achieved absolute, 100% decomposition within a 150-minute reaction window. [17]. Ameen et al. utilized a straightforward, solution-based approach to directly fabricate flower-like zinc oxide ZnO architectures using a zinc acetate precursor in an alkaline environment. Morphological analysis revealed that each individual ZnO flower structure was composed of distinct, well-defined petals possessing a mean

length of approximately  $\sim 300 \pm 50$  nm. The photocatalytic performance of these floral nano-architectures was subsequently evaluated by monitoring the breakdown of Crystal Violet dye under light exposure. The newly developed ZnO catalyst drove an exceptionally rapid decomposition of the target pollutant, eliminating roughly 96% of the CV dye within an 80-minute reaction period [18].

### III. MATERIALS AND METHODS

#### ➤ Preparation of Cobalt oxide $g\text{-C}_3\text{N}_4$ :

To synthesize the composite material, 5 g of  $\text{Co}(\text{NO}_3)_2 \cdot 6\text{H}_2\text{O}$  and 12 g of urea were thoroughly blended into a homogeneous mixture using a mortar and pestle, then transferred into a clean alumina crucible. To restrict gas dissipation during thermal processing, the crucible was tightly capped with its lid before being placed in a furnace for pyrolysis at  $400^\circ\text{C}$  for 2 h. After the furnace cooled down naturally to ambient room temperature, the crucible was retrieved. The resulting reddish-brown solid mass was then finely pulverized using an agate mortar and pestle to yield the sample designated as  $\text{CoO-g-C}_3\text{N}_4$ . For comparison, a pristine  $g\text{-C}_3\text{N}_4$  control sample was synthesized under identical thermal parameters by processing 10 g of pure urea, which yielded a characteristic pale-yellow powder.

### IV. CHARACTERIZATION OF COMPOSITE

#### ➤ EDX Spectrum:

The presence of cobalt oxide, carbon and nitrogen element was confirmed through an energy-dispersive X-ray spectroscopy. EDX spectrum of  $\text{CoO-g-C}_3\text{N}_4$  nanocomposite is given in Fig 1.

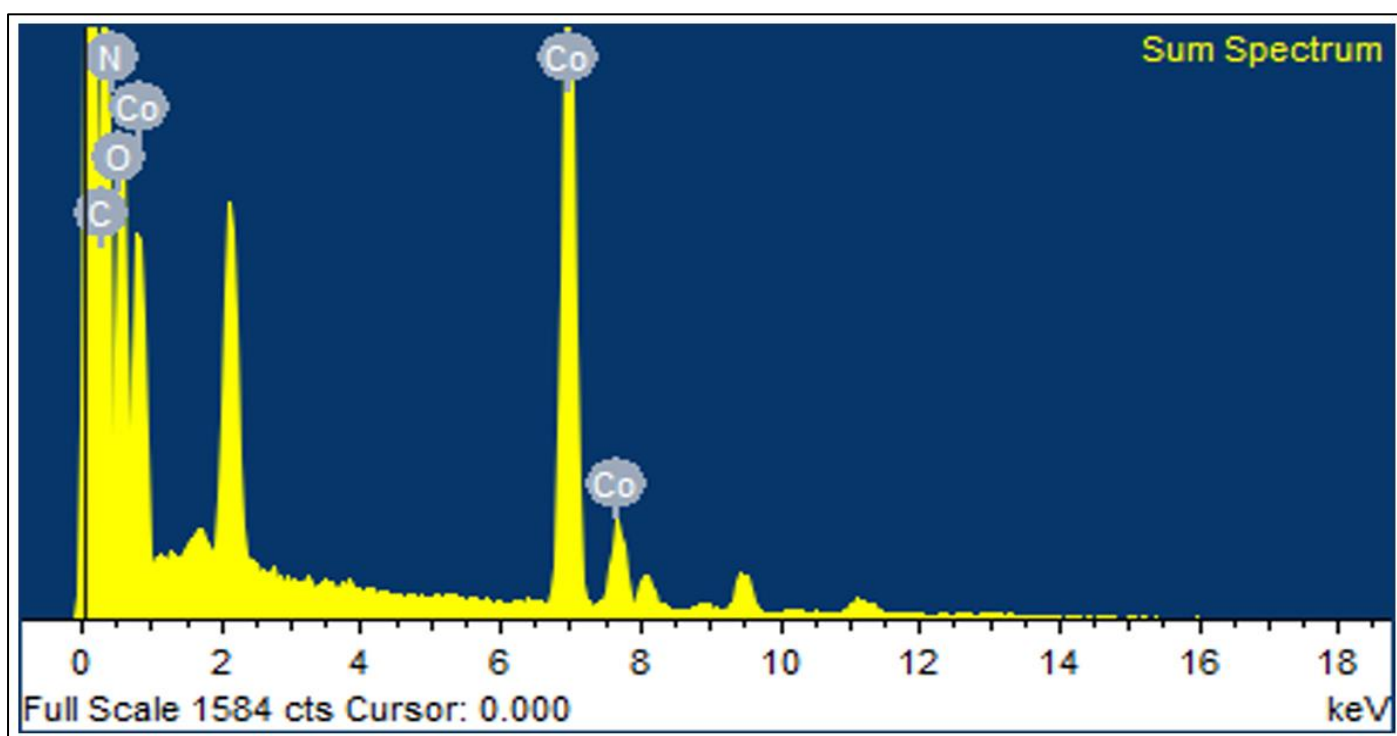


Fig 1 EDX Spectrum

➤ *FESEM Images:*

The field emission scanning electron microscopy analysis (FESEM) was performed. FESEM images of

different resolutions are given in Fig. 2. It shows porous nanoparticles with flower shape morphology

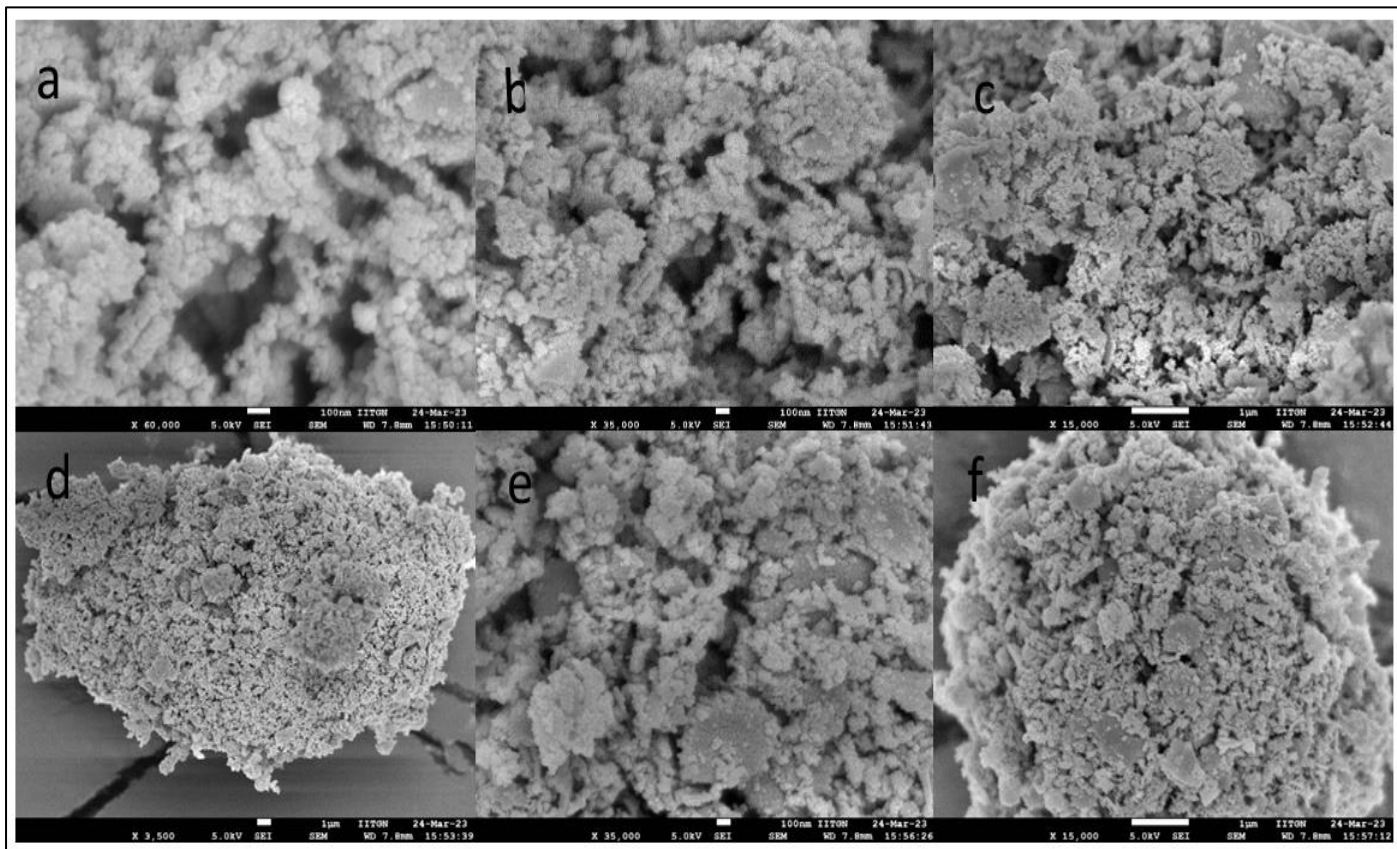


Fig 2 FESEM Images of CoO-g-C<sub>3</sub>N<sub>4</sub>

➤ *P-XRD:*

The crystalline integrity of the synthesized material was confirmed by the emergence of well-defined, sharp diffraction reflections in the X-ray diffraction (XRD) pattern.

To determine the average crystallite size of the engineered nanocomposite, the Debye–Scherrer mathematical model was applied to these peak profiles, yielding a mean crystallite dimension of 89.14 nm.

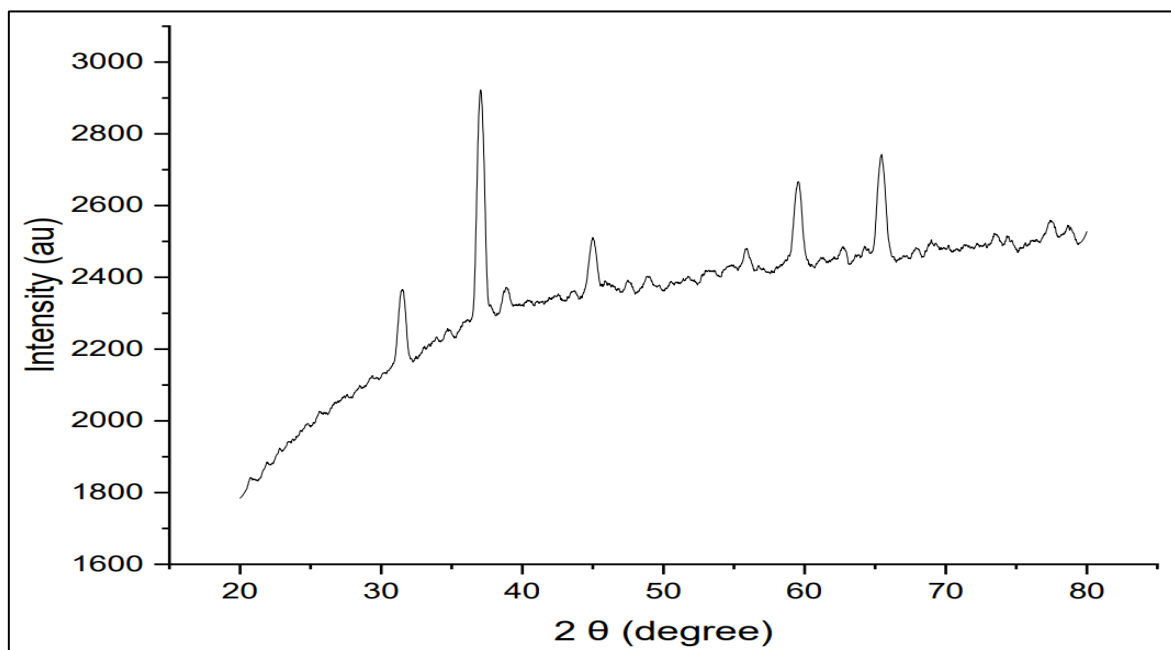


Fig 3 XRD Spectra

## V. STANDARD RUN

To prepare the primary stock solution with a concentration of  $1.0 \times 10^{-3}$  M, 0.0407 g of Crystal Violet dye was dissolved in 100 mL of double-distilled water. Aliquots from this master stock were subsequently diluted to achieve

the desired working concentrations. The optical absorbance (A) of the resulting solutions was monitored via spectrophotometry at a maximum absorption wavelength  $\lambda_{\max}$  590 nm. For the subsequent photocatalytic trials, uniform volumes of the prepared dye solution were distributed equally across six separate vessels as mentioned in table 1.

Table 1 Beaker Details

Vessels	Catalyst Type	Catalyst Dosage	Light Condition	Experimental Objective
1	None	0.00 g	Complete Dark	Dye stability check
2	None	0.00 g	Light Irradiation	Direct photolysis
3	Nanocomposite	0.08 g	Complete Dark	Equilibrium
4	Pristine g-C <sub>3</sub> N <sub>4</sub>	0.08 g	Light Irradiation	Baseline photocatalysis
5	cobalt oxide	0.08 g	Light Irradiation	Baseline photocatalysis
6	Nanocomposite	0.08 g	Light Irradiation	Targeted photocatalysis

Following a 3–4 h reaction period, the optical absorbance of each solution was quantified utilizing a UV-Vis spectrophotometer. The baseline controls (vessels 1–3) exhibited negligible changes, confirming that the dye remains stable in the dark or under light without a catalyst. Conversely, a moderate decline in initial absorbance was observed for the pristine g-C<sub>3</sub>N<sub>4</sub> and standalone cobalt oxide systems (vessels 4 and 5). Most notably, the mixture containing the engineered nanocomposite under light exposure (vessel 6) displayed the most pronounced attenuation in absorbance. These findings explicitly demonstrate that the degradation process is a synergistic mechanism, strictly requiring the simultaneous presence of both light irradiation and the composite catalyst.

Working solution of Crystal violet dye was arranged ( $2.0 \times 10^{-5}$  M) by diluting the stock solution and 0.08 g of synthesized CoO-g-C<sub>3</sub>N<sub>4</sub> nanocomposite and gCN was added to it for comparative study. The pH of reaction mixture was kept 8.0 and then this solution was exposed to a 200 W tungsten lamp at 60.0 mWcm<sup>-2</sup>. A spectrophotometer was utilized to monitor the optical absorbance of the Crystal Violet solution at its maximum absorption wavelength  $\lambda_{\max}$  590 nm. To prevent sample heating from disturbing the

reaction kinetics, a water-based optical filter was integrated into the path of the light beam to completely eliminate infrared and thermal radiation. Furthermore, the influence of light intensity on the photocatalytic process was systematically investigated by systematically varying the spatial distance separating the irradiation source from the catalyst-doped dye suspension. Absorbance of the solution at different time intervals was studied with the help of spectrophotometer. It was noted that the absorbance of the dye solution declines with raising time of exposure, which show decomposition of Crystal violet dye with time. The apparent pseudo-first-order rate constant k for the photocatalytic degradation process was calculated utilizing the linear relationship  $k = 2.303 \times \text{slope}$ . Based on this kinetic modelling, the observed reaction rate constant for the first-order decomposition pathway was determined to be  $4.54 \times 10^{-4}$  s<sup>-1</sup>.

The performance metrics obtained from these parallel evaluations are compiled comprehensively in Tables 2, 3, and 4. Additionally, a comparative graphic detailing the degradation trajectories driven by the synthesized composite, pristine g-C<sub>3</sub>N<sub>4</sub>, and standalone cobalt oxide is illustrated in Figure 4.

Table 2 Standard run with Nanocomposite [Crystal violet] =  $2.0 \times 10^{-5}$ , pH = 8.0, Nanocomposite = 0.08 g, Intensity of light = 60 mWcm<sup>-2</sup>

Time (min)	Absorbance A	1+ logA
0	0.829	0.9185
10	0.715	0.8543
20	0.594	0.7737
30	0.426	0.6294
40	0.351	0.5494
50	0.234	0.3692
60	0.162	0.2095

Rate constant (k) =  $4.54 \times 10^{-4}$ (s<sup>-1</sup>)

Table 3 Standard Run with g-C<sub>3</sub>N<sub>4</sub> [Crystal violet] =  $2.0 \times 10^{-5}$ , pH = 8.0, g-C<sub>3</sub>N<sub>4</sub> = 0.08 g, Intensity of light = 60 mWcm<sup>-2</sup>

Time (min)	Absorbance A	1+ logA
0	0.824	0.9159
10	0.725	0.8603
20	0.631	0.8000
30	0.534	0.7275
40	0.459	0.6618

50	0.388	0.5888
60	0.326	0.5132

Rate constant (k) =  $2.71 \times 10^{-4}(\text{s}^{-1})$

Table 4 Standard run with Cobalt Oxide [Crystal violet] =  $2.0 \times 10^{-5}$ , pH = 8.0, Cobalt oxide = 0.08 g, Intensity of light =  $60 \text{ mWcm}^{-2}$

Time (min)	Absorbance A	1+ logA
0	0.823	0.92
10	0.718	0.86
20	0.597	0.78
30	0.546	0.74
40	0.432	0.64
50	0.321	0.51
60	0.285	0.45

Rate constant (k) =  $2.95 \times 10^{-4}(\text{s}^{-1})$

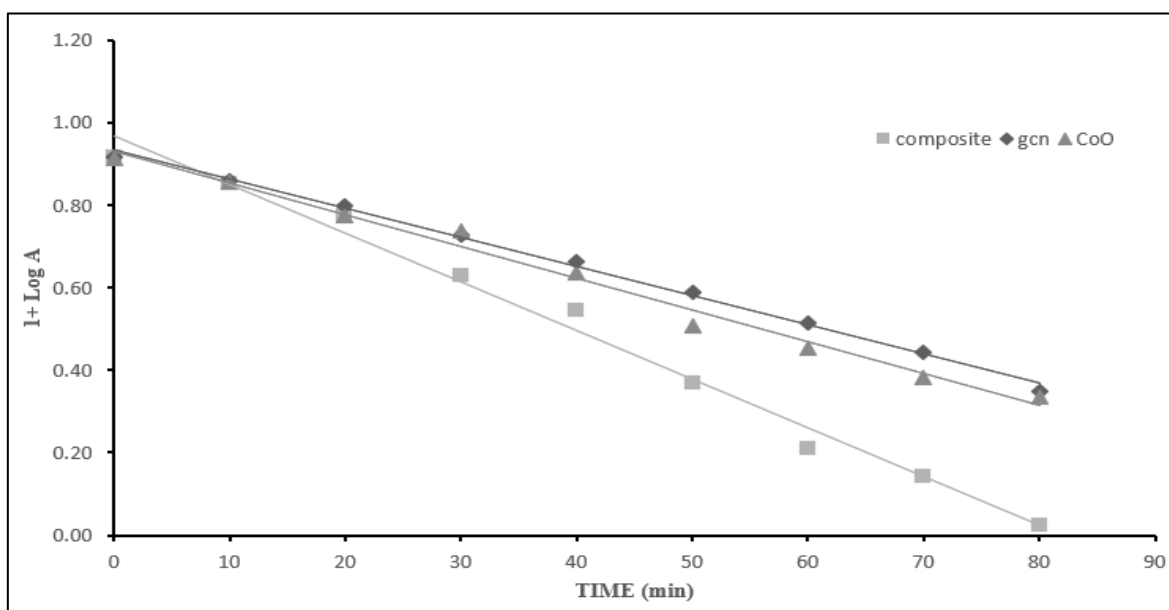


Fig 4 Standard Run Comparative Study

➤ pH Study:

The solution pH plays a critical role in dictating the photocatalytic decomposition kinetics of Crystal Violet. To evaluate this influence, the degradation velocity of the dye

was systematically investigated across a pH range of 6.5 to 10.0, with the corresponding experimental trends illustrated in Figure 5.

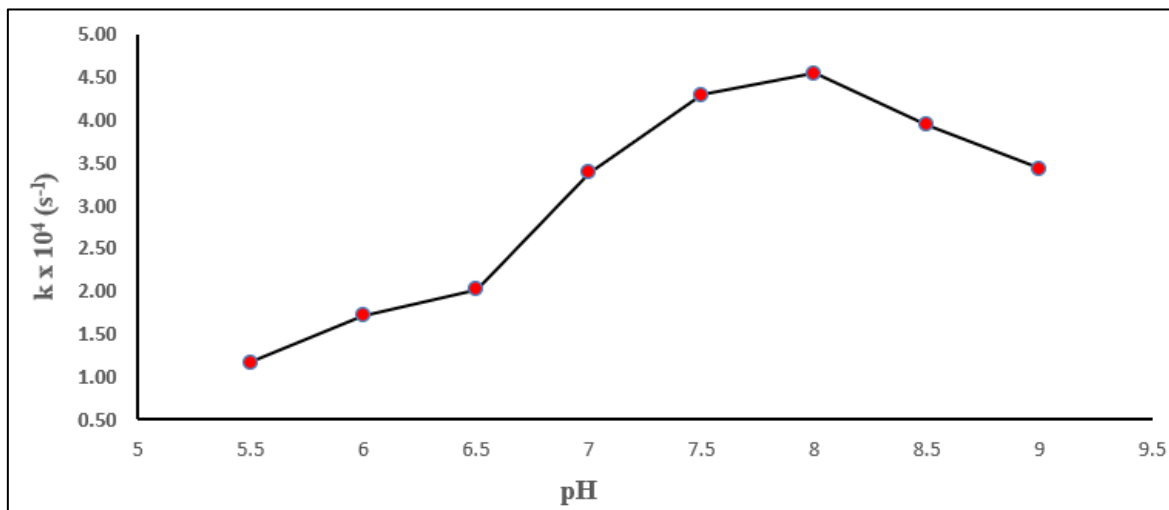


Fig 5 pH Study

The experimental data indicates that the dye degradation velocity escalates alongside rising pH levels, reaching a peak at pH 8.0. Beyond this threshold, further increments in alkalinity prompt a noticeable deceleration in the reaction rate. This unanticipated drop in performance can likely be attributed to chemical interactions between the basic medium and the dye molecules, which potentially triggers anion formation within the Crystal Violet structure. Conversely, the initial acceleration in degradation efficiency at higher pH values can be rationalised by the electronic dynamics of the system: dissolved oxygen molecules successfully intercept

photogenerated electrons from the conduction band of the photocatalyst. This trapping mechanism effectively stabilizes the holes ( $h^+$ ) in the valence band, thereby suppressing the rapid recombination of electron-hole pairs.

➤ *Concentration Study:*

To evaluate the influence of initial pollutant loading, the photocatalytic decomposition of Crystal Violet was systematically investigated across a concentration spectrum spanning  $0.5 \times 10^{-5}$  to  $3.0 \times 10^{-5}$  M. The resulting kinetic data and degradation profiles are graphically analysed in Figure 6.

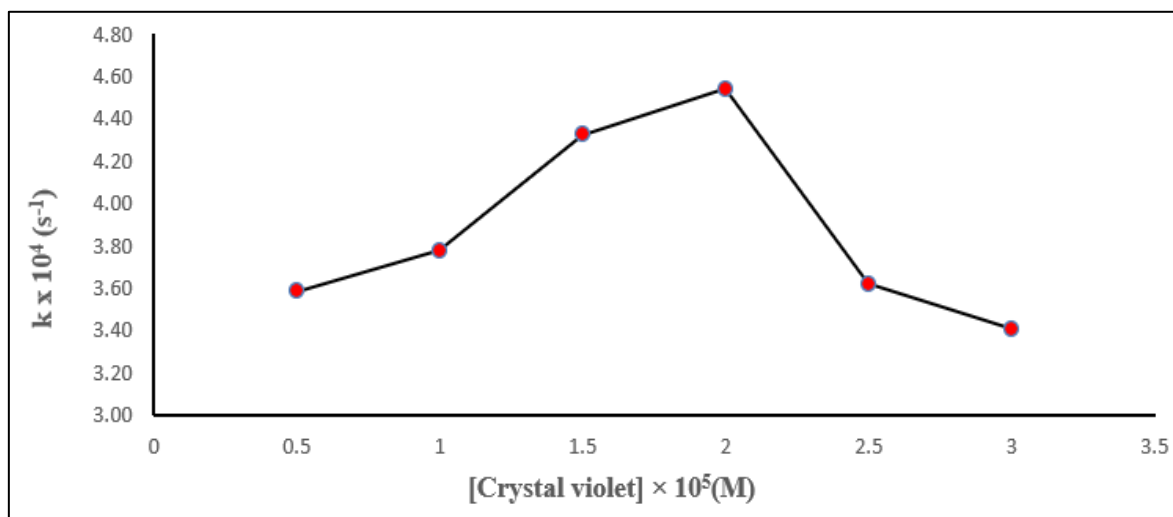


Fig 6 Concentration Study

The experimental results indicate that the photocatalytic breakdown velocity initially accelerates as the pollutant concentration rises. However, once the initial loading exceeds a threshold of  $2.0 \times 10^{-5}$  M, a distinct retardation in the decomposition rate is observed. The primary uptick in efficiency is ascribed to the higher availability of substrate molecules reacting near the active sites. Conversely, the sharp deceleration observed at concentrations above  $2.0 \times 10^{-5}$  M stems from the light-shielding effect of the dense dye solution; excessive pollutant molecules absorb the incoming

photons, thereby impeding the necessary light intensity from penetrating the suspension and activating the surface of the nanocomposite catalyst.

➤ *Effect of Amount of Composite:*

The influence of catalyst loading on the photocatalytic breakdown velocity was systematically evaluated by varying the mass of the nanocomposite from 0.02 to 0.12 g. The corresponding experimental profiles and trends are illustrated in Figure 7.

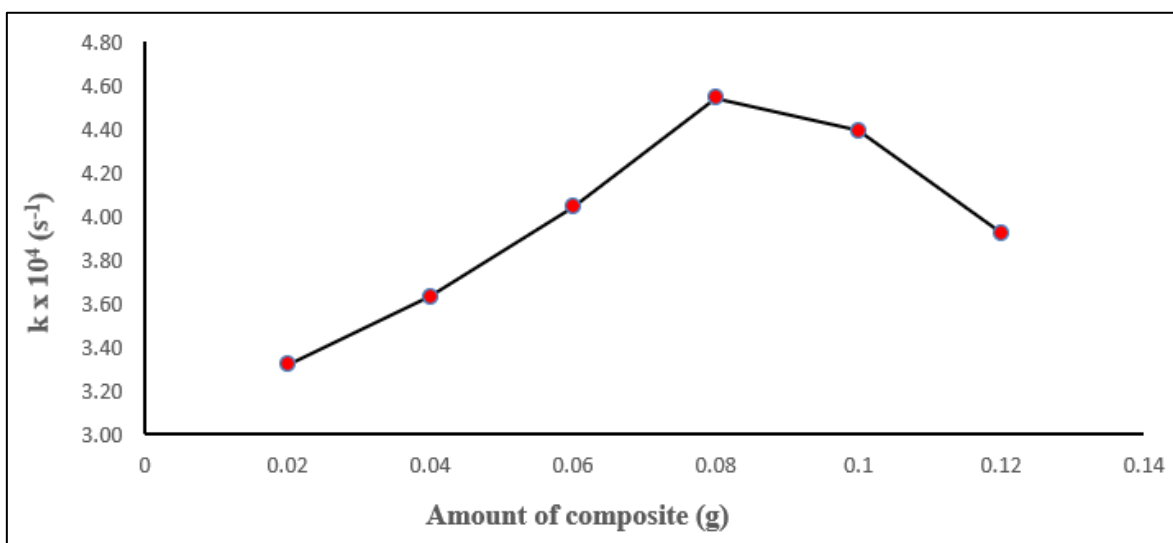


Fig 7 Composite Amount Study

The experimental profiles demonstrate that scaling up the catalyst dosage yields a corresponding increase in photocatalytic efficiency. The decomposition velocity peaked at an optimal nanocomposite loading of 0.08 g beyond which a distinct downward trend in the reaction rate was observed. The initial acceleration in dye breakdown can be ascribed to the progressive expansion of the available active surface area up to the 0.08 g threshold. Conversely, adding mass past this optimum point does not provide additional exposed active sites; instead, it merely thickens the catalyst layer and promotes particle agglomeration. This physical limitation, which induces light-scattering and prevents photons from penetrating the deeper layers of the suspension, was explicitly

verified by performing parallel control trials in reaction vessels of varying geometric dimensions.

➤ *Intensity of Light Study:*

To evaluate the impact of photon flux on the photocatalytic decomposition process, the spatial distance between the irradiation source and the exposed surface of the nanocomposite suspension was systematically adjusted. Through these adjustments, the incident light intensity was varied across a range from 20 to 70 mWcm<sup>-2</sup>. The corresponding experimental data and kinetic trends are graphically illustrated in Figure 8.

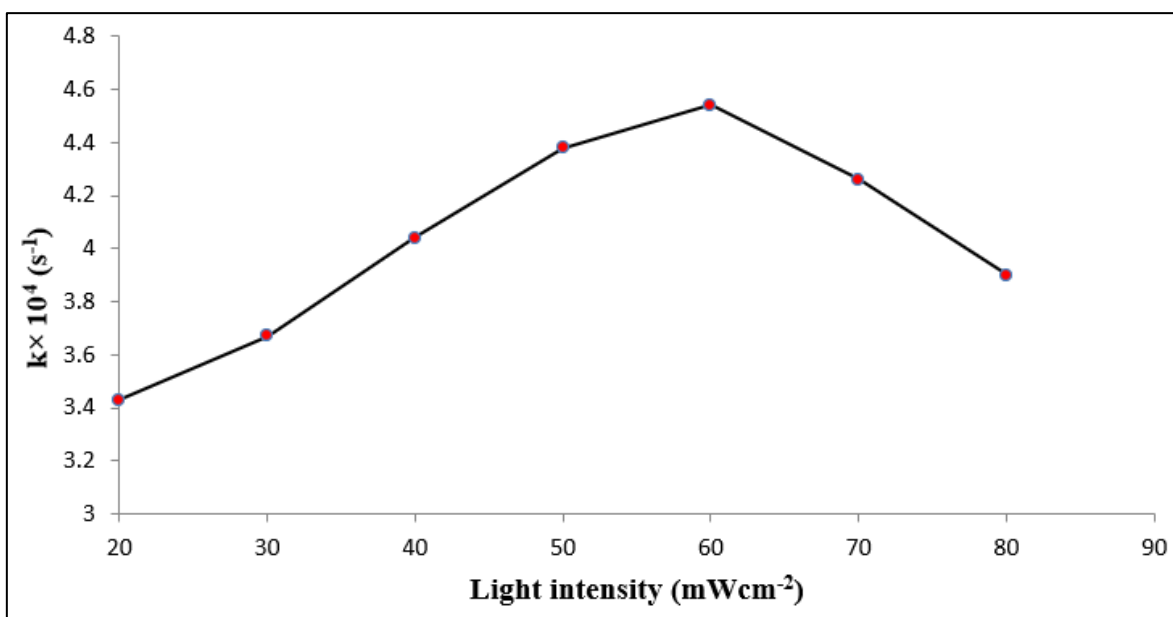
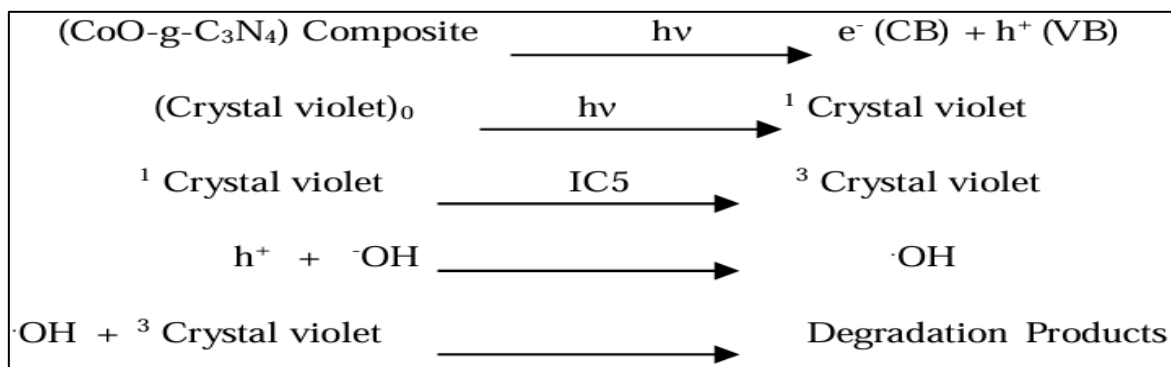


Fig 8 Intensity of Light Study

The experimental data indicates that the dye decomposition rate elevates monotonically with increasing light intensity. This acceleration is primarily ascribed to the heightened photon flux interacting with the photocatalyst surface, which significantly promotes the generation of photogenerated excitons (electron-hole pairs). However, under elevated irradiation intensities, localized thermal side-reactions can occur within the system; these temperature-driven pathways disrupt the desired photocatalytic mechanism, ultimately leading to a marginal retardation in the overall degradation efficiency.

➤ *Mechanism*

The mechanism proceeds through the following sequential charge-transfer steps:



Here the light (hv) excites e<sup>-</sup> from valence band (VB) of the composite to conduction band (CB) creates hole (h<sup>+</sup>) at the valence band. And same time dye is also excited to the

singlet state and then converted to triplet state (<sup>3</sup> Crystal violet). The h<sup>+</sup> combines with hydroxyl ions (^-OH) on the surface of photocatalyst to produce hydroxyl radical (^·OH).

Then the  $\cdot\text{OH}$  degrade the dye molecules. The reactive species is  $\cdot\text{OH}$  which was confirmed by observing the reaction in the presence of scavenger 2-propanol where the rate is

substantially decreased. Also, the rate remarkably decreases for ammonium oxalate (AO) as  $\text{h}^+$  scavenger because  $\text{h}^+$  is responsible for produce the  $\cdot\text{OH}$ .

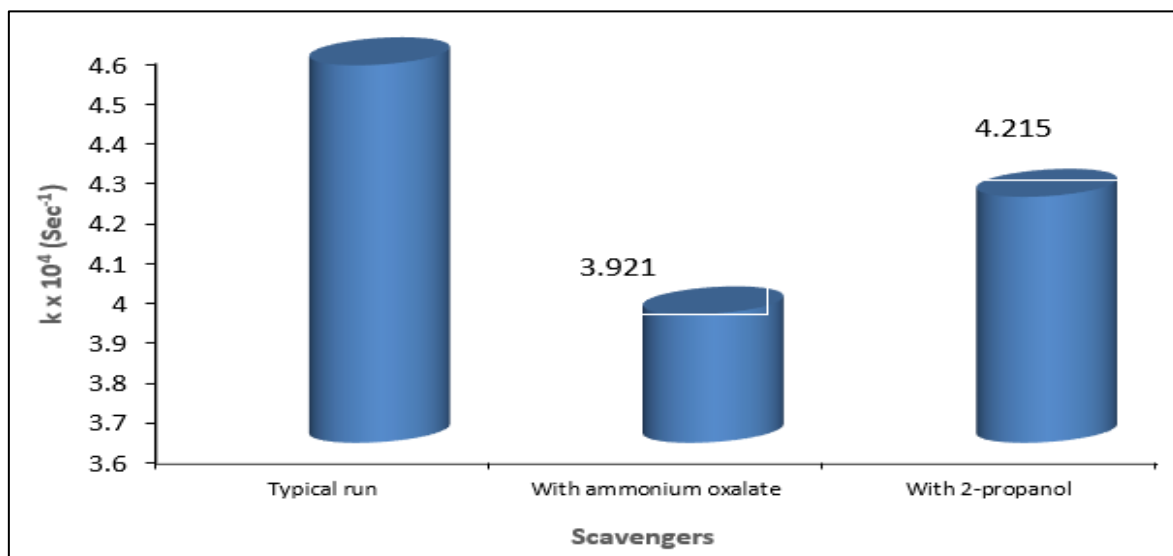


Fig 9 Scavengers vs Rate Constant

## VI. CONCLUSION

The CoO-g-C<sub>3</sub>N<sub>4</sub> nanocomposite was synthesized successfully. It was characterised by EDX, FESEM and p-XRD. The synthesized nanocomposite studied successfully for photocatalytic degradation of Crystal violet dye under visible light. Different parameter was studied like pH, concentration of dye, amount of nanocomposite, light intensity. With optimized parameters the Crystal violet dye degraded efficiently. Mechanism investigation clearly indicates that reactive species is  $\cdot\text{OH}$  which involve in the degradation of dye. So, CoO-g-C<sub>3</sub>N<sub>4</sub> nanocomposite can be used as photocatalyst for degradation of different dyes and organic contaminants in water. It will help to treatments of polluted water and increasing the recyclability of water.

## ACKNOWLEDGMENTS

The author is thankful to Head, Department of Chemistry Pacific university, Udaipur for providing necessary laboratory facilities.

### ➤ Conflict of Interest

Authors declares that they have no conflict of interest.

## REFERENCES

- [1]. T. Robinson, B. Chandran and P. Nigam, "Studies on desorption of individual textile dyes and a synthetic dye effluent from dye-adsorbed agricultural residues using solvents", *Bioresource Technology*, vol. 84(3), pp. 299-301, 2002.
- [2]. I. Ahmed, M. H. M. N. Iqbal and K. Dhama, "Enzyme based biodegradation of hazardous pollutants- an overview", *Journal of Experimental Biology and Agricultural Sciences*, vol.5(4), pp. 403-411, 2017.
- [3]. A. Anandan, G. Rajiv, R. Eswaran and M. Prakash, "Genotypic variation and relationships between quality traits and trace elements in traditional and improved rice genotypes", *Journal of Food Science*, vol.76(4), pp. 122-130, 2011.
- [4]. D. Jiang, T. Otitoju, Y. Ouyang, N. Shoparwe and S. Wang, "A Review on Metal Ions Modified TiO<sub>2</sub> for Photocatalytic Degradation of Organic Pollutants", *Catalysts*, vol. 11(9), pp. 1039, 2021.
- [5]. J., Jia, Q. Zhang, K. Li, Y. Zhang, E. Liu and X. Li, "Recent advances on g-C<sub>3</sub>N<sub>4</sub>-based Z-scheme photocatalysts: Structural design and photocatalytic applications", *International Journal of Hydrogen Energy*, vol.48(1), pp. 196-231, 2023.
- [6]. S. Cao, J. Low, J. Yu, and M. Jaroniec, "Polymeric photocatalysts based on graphitic carbon nitride. *Advanced Materials*", vol. 27(13), pp. 2150-2176, 2015.
- [7]. L. Wang, C. Wang, X. Hu, H. Xue, and H. Pang, "Metal/graphitic carbon nitride composites: Synthesis, structures, and applications", *Chemistry–An Asian Journal*, vol. 11(23), pp. 3305-3328, 2016.
- [8]. P. Praus, L. Svoboda, M. Ritz, I. Troppova, M. Sihor, and K. Kocí, "Graphitic carbon nitride: Synthesis, characterization and photocatalytic decomposition of nitrous oxide", *Materials Chemistry and Physics*, vol. 193, pp. 438-446, 2017.
- [9]. H. An, , N. M. Dat, N.D. Hai, C.Q. Cong, N.T. H. Nam, L. T. Tai, and N. H. Hieu, "Photocatalytic degradation of organic dyes using zinc oxide-decorated graphitic carbon nitride composite under visible light", *Diamond and Related Materials*, vol. 131, pp. 109583, 2023.
- [10]. C. R. Dhas, R. Venkatesh, K. Jothivenkatachalam, A. Nithya, B. S. Benjamin, and A. M. E. Raj, "Visible light driven photocatalytic degradation of Rhodamine B and Direct Red using cobalt oxide

- nanoparticles. *Ceramics International*”, vol. 41(8), pp. 9301-9313, 2015.
- [11]. S. Farhadi, M. Javanmard and G. Nadri, “Characterization of cobalt oxide nanoparticles prepared by the thermal decomposition”, *Acta Chimica Slovenica*, vol. 63(2), pp. 335-343, 2016.
- [12]. A. B. Asif, S. B. Khan and A. M. Asiri, “Efficient solar photocatalyst based on cobalt oxide/iron oxide composite nanofibers for the detoxification of organic pollutants”, *Nanoscale research letters*, vol. 9, pp. 1-9, 2014.
- [13]. S. P. Pattnaik, A. Behera, S. Martha, R. Acharya, and K. Parida, “Facile synthesis of exfoliated graphitic carbon nitride for photocatalytic degradation of ciprofloxacin under solar irradiation”, *Journal of Materials Science*, vol. 54(7), pp. 5726-5742, 2019.
- [14]. Y. Cui, Y. Tang, and X. Wang, “Template-free synthesis of graphitic carbon nitride hollow spheres for photocatalytic degradation of organic pollutants”, *Materials Letters*, vol. 161, pp. 197-200, 2015.
- [15]. F. A. Alshamsi, A. S. Albadwawi, M. M. Alnuaimi, M. A. Rauf, and S. S. Ashraf, “Comparative efficiencies of the degradation of Crystal Violet using UV/hydrogen peroxide and Fenton's reagent”, *Dyes and pigments*, vol. 74(2), pp. 283-287, 2007.
- [16]. C. Sahoo, A. K. Gupta, and A. Pal, “Photocatalytic degradation of Crystal Violet (CI Basic Violet 3) on silver ion doped TiO<sub>2</sub>”, *Dyes and Pigments*, vol. 66(3), pp. 189-196, 2005.
- [17]. W. Ahmad, A. Khan, N. Ali, S. Khan, S. Uddin and S. Malik, “Photocatalytic degradation of crystal violet dye under sunlight by chitosan-encapsulated ternary metal selenide microspheres”, *Environmental Science and Pollution Research*, vol. 28, pp. 8074-8087, 2021.
- [18]. S. Ameen, M. S. Akhtar, M. Nazim, and H. S. Shin, “Rapid photocatalytic degradation of crystal violet dye over ZnO flower nanomaterials”, *Materials letters*, vol. 96, pp. 228-232, 2013.